Computerized Measurement of Myocardial Infarct Size on Contrast-Enhanced Magnetic Resonance Images

Li-Yueh Hsu*, Peter Kellman, Alex Natanzon, Glenn A. Hirsch, Anthony H. Aletras, Andrew E. Arai

Laboratory of Cardiac Energetics, National Heart Lung and Blood Institute, National Institute of Health, Bethesda, MD 20892-1061

ABSTRACT

Purpose: To validate a computer algorithm for measuring myocardial infarct size on gadolinium enhanced MR images. The results of computer infarct sizing are studied on phase-sensitive and magnitude imaging against a histopathology reference. *Materials and Methods:* Validations were performed in 9 canine myocardial infarctions determined by triphenyltetrazolium chloride (TTC). The algorithm analyzed the pixel intensity distribution within manually traced myocardial regions. Pixels darker than an automatically determined threshold were first excluded from further analysis. Selected image features were used to remove false positive regions. A threshold 50% between bright and dark regions was then used to minimize partial volume errors. Post-processing steps were applied to identify microvascular obstruction. Both phase sensitive and magnitude reconstructed MR images were measured by the computer algorithm in units of % of the left ventricle (LV) infarction and compared to TTC. *Results:* Correlations of MR and TTC infarct size were 0.96 for both phase sensitive and magnitude imaging. Bland Altman analysis showed no consistent bias as a function of infarct size. The average error of computer infarct sizing was less than 2% of the LV for both reconstructions. Fixed intensity thresholding was less accurate compared to the computer algorithm. *Conclusions:* MR can accurately depict myocardial infarction. The proposed computer algorithm accurately measures infarct size on contrast-enhanced MR images against the histopathology reference. It is effective for both phase-sensitive and magnitude imaging.

Keywords: myocardial infarction, magnetic resonance imaging, computer quantification

1. INTRODUCTION

Gadolinium delayed enhancement MR methods for imaging myocardial infarction are becoming widely used. Although a high correlation between ex vivo imaging and triphenyltetrazolium chloride (TTC) images has been shown (1,2), quantitative validation at the resolution used in vivo against TTC has not been studied. We aimed to develop a computer algorithm that objectifies in vivo myocardial infarction (MI) measurements and can be generalized to different MR reconstruction schemes, i.e. phase-sensitive and magnitude. The performance of the algorithm was evaluated using both reconstruction methods and compared to the TTC reference standard.

Measurement of myocardial infarction on contrast-enhanced MR images is typically performed by manual planimetry and with computer fixed intensity thresholding. Expert human interpretation can vary depending on the computer window and level display setting that may increase or decrease the conspicuity of different signal intensity regions. Although fixed threshold techniques reduce inter- or intra-observer variability, they lack robustness due to use of empirical thresholds. For example, Setser et al (3) allowed the user to set a threshold to separate the normal myocardium from the infarct. Other studies have used thresholds ranging from 2 to 6 standard deviations brighter than normal myocardium as a way to discriminate infarcted from non-infarcted myocardium (1-8). Considering the error introduced by partial volume effects, an alternative threshold based on 50% of the maximum intensity may be desirable. In addition to fixed numerical thresholding methods, the expert human uses empirical qualitative

* Correspondence: lyhsu@nhlbi.nih.gov; Phone: (301) 496-3658; Fax: (301) 402-2389

approaches to decide where to segment the border of a myocardial infarction. One example of this would be ignoring random bright pixels or moderate-sized patches interpreted to represent RV blood as opposed to an atypical epicardial infarct.

Computer algorithms that could objectively analyze infarct size with user independent selected thresholds, and image processing techniques that use feature analysis to reduce false positive infarct region would be beneficial, particularly if they were applied to images acquired with practical in vivo resolution. We addressed three basic hypotheses in this study. First, segmentation based only on the distribution of signal intensity values of normal myocardium will tend to overestimate infarct size relative to objective segmentation approaches that use an optimal threshold between bright and dark regions, such as 50% of the maximum intensity described in this paper. Second, advanced image processing techniques can further refine the accuracy of measuring infarct size by using rules derived from expert readers. For example, myocardial infarction is most likely to start in the subendocardium and extend toward the epicardium. Patches of bright pixels smaller than a certain size are more likely to represent artifacts than larger patches. Three-dimensional connectivity with neighboring bright patches can also be used to increase the likelihood that a region is part of the infarct. Third, computer measured infarct size will be comparable in inversion recovery imaging irregardless of different reconstruction methods provided that myocardial signal intensity is optimally nulled. These hypotheses were tested in a canine infarct model with triphenyltetrazolium chloride as the histopathological reference standard.

2. MATERIALS AND METHODS

Nine mongrel dogs were imaged on a 1.5T scanner (GE Medical Systems) approximately 20-30 minutes following administration of Gd-DTPA. Myocardial infarction was induced by a 90 minute left anterior descending coronary artery occlusion and followed by reperfusion. Typical imaging parameters included TE 3.4 ms, TR 7.8 ms, bandwidth ±31.25 kHz, and acquisition time 94 ms per R-R interval, which achieved a spatial resolution of 1.1x1.8x8.0 mm in vivo. Histopathological triphenyltetrazolium chloride (TTC) stained images were prepared and photographed at 4 mm intervals after cutting the heart with a commercial meat slicer. The area of infarction was determined by manual planimetry of negative TTC staining on the images and reported in units of percentage of the left ventricle (LV) myocardial region.

With in inversion recovery imaging technique, the myocardial signal intensity is nulled by using proper inversion time such that normal myocardial regions contain noise only. In addition to the existence of noise in the myocardium, the receiving coil also has an inhomogeneous magnetic field that imposes signal intensity variation over the myocardial region of interest. This not only produces an inconsistent signal intensity on the dark normal myocardium, it also affects the maximum intensity measurement on the bright infarcted region. To minimize these intensity inconsistencies, all MR images in our experiment were acquired by selecting an optimal inversion time during the acquisition. Both phase-sensitive (9) and magnitude inversion recovery reconstructions were performed. A reference image was also obtained with a small flip angle (proton density weighted) to measure the surface coil signal intensity variation. Both phase-sensitive and magnitude images were processed using this reference image for intensity correction (Figure 1).

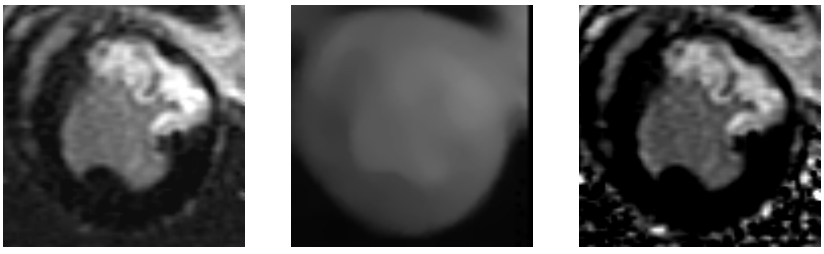

Figure 1. Example of delayed enhancement MR images before (left) and after (right) the surface coil intensity correction. Using a reference image (middle), the image after the correction shows more homogeneous dark normal myocardial regions. Bight infarct area at anterior-lateral region also shows more consistent intensity after the correction.

For MR image processing, the contours of epicardium and endocardium of all images were first manually traced by a human observer using a custom image display and analysis tool. The computer algorithm then applied a series of pre-determined steps to classify infarct and normal regions (Figure 2). The algorithm automatically estimates an initial threshold to separate the infarction from the normal myocardium. Both median filtering and histogram clustering are used to smooth the random noise on the spatial and the histogram spaces before the threshold estimation.

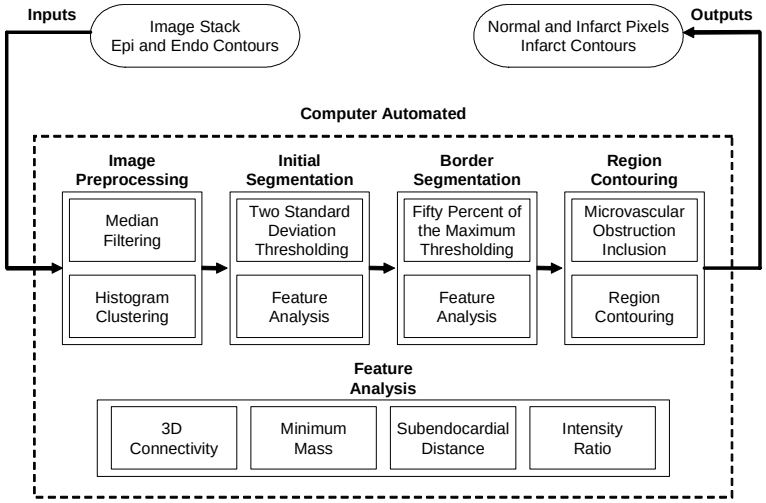

Figure 2. Flow diagram of the computer myocardial infarct sizing algorithm.

Two Standard Deviation Thresholding: The mean and standard deviation of the normal tissue is first estimated by the maximum value of the lower part of the intensity histogram. The threshold value is then calculated using a two standard deviation distance above the mean. Pixels darker than this threshold value are excluded from further analysis. This, however, leaves aggregates of bright pixels that included infarct, imperfectly excluded pixels of epicardial fat or right ventricular blood, randomly bright pixels, and artifacts. An initial threshold set at two standard deviations above the mean may seem relatively low since it covers 95% of a normal distribution. However, it is desirable to maintain a lower threshold to increase the probability of detecting more bright infarcts and then discounting false infarct pixels during follow up processing.

Region Based Feature Analysis: To remove false positive pixels, the following image features are computed and classified on each aggregated potential infarct region in 3D space: volume mass, subendocardial distance, and mean intensity. Before the feature analysis, all slices are registered to the center of the myocardial regions of interest. This ensures a proper 3D propagation of myocardial regions through the entire image stack. To calculate the infarct mass, all potential 2D regions are first grouped to 3D volumes using connected component analysis. This technique aggregates isolated 2D regions into 3D volumes based on the definition of neighbor connectivity. We implement 10-neighbor connectivity based on the large slice thickness of our dataset. After the process, each potential 3D volume is then converted to units of mass based on the density of myocardium (1.05 g/mm^3). Any bright volume that has a mass smaller than a minimum setting (0.1 g) is considered as noise and removed. To obtain the subendocardial distance, the shortest path of each potential 3D infarcted volume to the endocardial boundary is computed amongst all border pixels. Any bright volume more than 2 mm away from the endocardial border is considered an artifact and removed. Additionally, the intensity value of each potential 3D volume is examined for homogeneity. For each volume, the mean intensity value is computed as a ratio to the average intensity of all potential infarcted volumes. A minimum setting of 50% is used to remove volumes that have a darker average intensity.

Fifty Percent of the Maximum Thresholding: While the above steps effectively remove disjointed false positive bright regions, overestimation of infarct size is still possible due to the tissue partial volume effect. The next step is to determine a final threshold to classify partial volume tissues. We use 50% of the maximum intensity

threshold calculated as the mid point between the normal myocardium and peak infarct tissue intensities. In delayed enhancement imaging, the normal myocardial signal is optimally nulled using a proper inversion recovery time and thus contains noise only. For phase-sensitive reconstruction, the mean intensity of the normal myocardium is estimated from the peak value of the lower part of the intensity histogram since the mean value is unbiased. For magnitude imaging, a value of zero was used to define the normal myocardium signal intensity, on the assumption the inversion time was correctly selected to null normal myocardium. This 50% value represents a contour delineation threshold setting for candidate partial infarcted regions. Any residual bright pixels less than this value are excluded from the infarct region of interest. After the thresholding, the region based feature analysis is performed again to further reduce false positive infarct regions.

Microvascular Obstruction Inclusion: Additional post-processing steps are applied to take account of dark pixel regions that may represent microvascular obstruction. An image morphology closing operation with a crossbar shape kernel is used to connect small concave borders and fill small dark cavities surrounded by bright infarcted pixels. A small kernel (5 mm) of such process can also smooth the border of infarct regions without excessively altering the overall shape. Next, remaining regions of isolated dark pixels are further analyzed to identify possible areas of microvascular obstruction. Each dark region is reclassified as infarct if its border is completely encompassed by either endocardial or infarct pixels. These processes compensate for dark areas of microvascular obstruction that are too low a signal intensity to be detected by the thresholding steps. Finally, an edge following step is applied to obtain the contour of infarcted regions for qualitative representation.

3. RESULTS

Figure 3 shows the correlation and Bland Altman plots of infarct size between TTC, as a reference standard, and MRI. Both phase-sensitive and magnitude imaging show good correlations and Bland Altman analysis confirms no consistent bias as a function of infarct size exists. Figure 4 shows the effect of varying the intensity threshold in the final contour delineation step. The minimum percentage error of MI size occurs when the final contouring threshold is set at 50% of the maximum intensity. Use of lower thresholds systematically overestimated infarct size while higher thresholds underestimated infarct size (figure 4). The average error in infarct size determination was less than 2.0% for both reconstruction techniques.

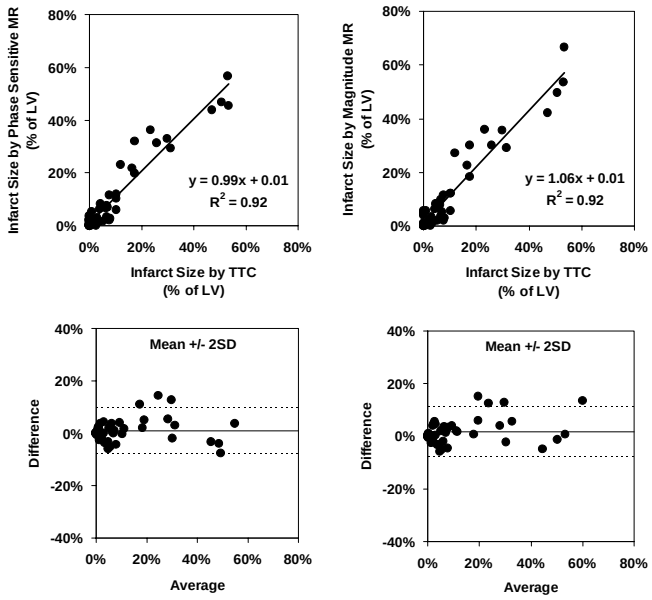

Figure 3. Correlation and Bland-Altman analysis of MI size determined by the computer algorithm against histopathology reference standard. Both phase sensitive (left) and magnitude (left) results are shown.

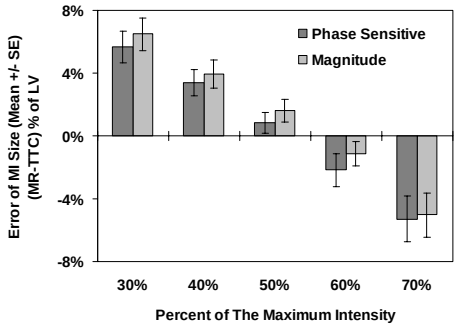

Figure 4. Analysis of the maximum intensity thresholding step in the computer algorithm. The optimal setting was found at 50% of the maximum intensity.

Figure 5 shows the infarct size measured from the computer algorithm and different thresholding methods for all MR images and the TTC reference standard. The results were compared using the difference (as the error) of percentage of LV infarct area between MR and TTC images. For the group data overall, the fifty percent of the maximum thresholding produced a smaller error than the two standard deviation thresholding ($p<0.001$). However, the computer algorithm further reduced the error compared to both simply intensity thresholding techniques.

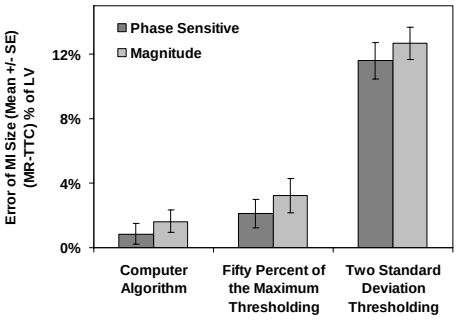

Figure 5. Average errors of infarct size measurement in units of percent of the LV mass for phase sensitive and magnitude MR images. The computer algorithm produces less than 2% average error for both phase sensitive and magnitude images. Fixed thresholding methods (fifty percent of the maximum and two standard deviation) consistently overestimated the infarct size compared to the computer algorithm.

4. DISCUSSION

To objectively measure the size of myocardial infarction on contrast-enhanced MR images, a computer algorithm was developed that automatically selects optimal thresholds and uses feature analysis methods to classify normal and infarcted myocardial regions. The algorithm accurately measured infarct size on in vivo MR images and reduced interobserver variability. Completely manual traces, despite strong correlations versus TTC, had a tendency to overestimate infarct size on MR images.

While quantitative analysis of contrast-enhanced MR using fixed intensity thresholding generally reduced intra- or interobserver variability and enhanced the reproducibility in prior studies, such threshold based techniques lack robustness due to empirical threshold setting and may overestimate infarct size by inclusion of all bright pixels. Since image resolution and partial volume effects have been implicated as a potential source of error in infarct quantification (10-12), it is important to consider the intensity thresholds used to discriminate infarcted from normal myocardium. In fact, the thresholds selected from previous studies (1-8) have ranged from 2 to 6 standard deviations

based on the normal myocardium and have generally not considered the distribution of signal intensities in the infarcted myocardium.

The computer algorithm incorporating region based feature analysis improves results compared with fixed thresholding methods. The region based feature analysis motivated by clinical knowledge encompasses computer rules to analyze the patterns of bright image pixels and subsequently increases or decreases the probability of bright pixel blobs being true positive infarcts. Our study demonstrated that automatically estimated thresholds combined with region based feature analysis effectively minimized type-II misclassification errors (false positive; overestimation) that occurred in fixed thresholding techniques. The benefit of computer feature analysis is most evident for eliminating epicardial white patches, such as right ventricular blood, that are included within imperfectly drawn epicardial traces. It also can exclude small isolated bright blobs that result from imaging noise or artifacts provided they were not connected in 3D space with other areas of infarction.

The fifty percent of the maximum intensity thresholding part of the algorithm most directly addresses the inevitable partial volume effects that are encountered in vivo and clinically. It is important to recognize that partial volume effects will be most severe in the transmural direction of the left ventricular wall rather than the circumferential direction. This is important since the clinical validation studies indicate transmural resolution is one of the significant advantages of MR imaging over other non-invasive techniques (5,13). From the perspective of overall errors, partial volume effects will be most prominent as the number of imaging voxels on the border of the infarct increases relative to the size of the infarct core. The use of fifty percent of the maximum infarct intensity threshold, as opposed to the threshold based on two standard deviations of the normal myocardium, can more accurately dichotomize normal from infarcted voxels when partial volume effects are significant.

However, the fifty percent of the maximum intensity thresholding, like all fixed thresholding techniques, is still subject to the influence of imaging artifacts and human errors in tracing epicardial and endocardial borders. The benefits of adding image processing and feature analysis to the computer algorithm are considerable in our study. The region based feature analysis removes false positive bright pixels miscategorized as infarcted tissue by fixed thresholding methods. It reduces the average errors of two standard deviation and fifty percent of the maximum intensity thresholding techniques. Overall, the most accurate infarct measurement was achieved using the complete computer algorithm. This is true for both phase-sensitive and magnitude image reconstructions.

5. CONCLUSIONS

This paper provides a documentation that both phase sensitive and properly nulled magnitude inversion recovery imaging can accurately depict the infarct region in vivo against histopathological reference standard. Using a computer algorithm optimized to automatically select intensity thresholds and perform image feature analysis, myocardial infarct size can be accurately measured in both imaging methods. The algorithm produces high correlations with the reference standard and decreases type-II misclassification errors introduced by conventional fixed intensity thresholding techniques. It may also minimize intra- and interobserver variability, and reduces systematic overestimation that plagues human manual measurements.

REFERENCE

1. R.J. Kim, D.S. Fieno, R.B. Parrish, et al., “Relationship of MRI delayed contrast enhancement to irreversible injury, infarct age, and contractile function,” *Circulation.* **100**, pp. 1992-2002, 1999.
2. D.S. Fieno, R.J. Kim, E.L. Chen, J.W. Lomasney, F.J. Klocke, R.M. Judd, “Contrast-enhanced magnetic resonance imaging of myocardium at risk: distinction between reversible and irreversible injury throughout infarct healing,” *J. Am. Coll. Cardiol.* **36**, pp. 1985-1991, 2000.
3. R.M. Setser, D.G. Bexell, T.P. O'Donnell, et al., “Quantitative assessment of myocardial scar in delayed enhancement magnetic resonance imaging,” *J. Magn. Reson. Imaging.* **18,** pp. 434-441, 2003.

4. G.K. Lund, A. Stork, M. Saeed, M.P. Bansmann, J.H. Gerken, V. Muller, J. Mester, C.B. Higgins, G. Adam, T. Meinertz, "Acute myocardial infarction: evaluation with first-pass enhancement and delayed enhancement with MR imaging compared with 201ST1 SPECT imaging," *Radiology*. **232,** pp. 49-57, 2004.
5. R.J. Kim, E. Wu, A. Rafael, et al., "The use of contrast-enhanced magnetic resonance imaging to identify reversible myocardial dysfunction," *N. Engl. J. Med.* **343**, pp. 1145-1453, 2000.
6. H.B. Hillenbrand, R.J. Kim, M.A. Parker, D.S. Fieno, R.M. Judd, "Early assessment of myocardial salvage by contrast-enhanced magnetic resonance imaging," *Circulation*. **102**, pp. 1678-1683, 2000.
7. H. Mahrholdt, A. Wagner, T.A. Holly, et al., "Reproducibility of chronic infarct size measurement by contrast-enhanced magnetic resonance imaging," *Circulation.* **106**, pp. 2322-2327, 2002.
8. E.C. Perin, G.V. Silva, R. Sarmento-Leite, et al., "Assessing myocardial viability and infarct transmurality with left ventricular electromechanical mapping in patients with stable coronary artery disease: validation by delayed-enhancement magnetic resonance imaging," *Circulation*. **106**, pp. 957-961, 2002.
9. P. Kellman, A.E. Arai, E.R. McVeigh, A.H. Aletras, "Phase sensitive inversion recovery for detecting myocardial infarction using Gadolinium delayed hyperenhancement," *Magn. Reson. Med.* **47**, pp. 362-383, 2002.
10. M.R. Goldman, T.J. Brady, I.L. Pykett, et al., "Quantification of experimental myocardial infarction using nuclear magnetic resonance imaging and paramagnetic ion contrast enhancement in excised canine hearts," *Circulation*. **66**, pp. 1012-1016, 1982.
11. R.M. Judd, C.H. Lugo-Olivieri, M. Arai, et al., "Physiological basis of myocardial contrast enhancement in fast magnetic resonance images of two-day old reperfused canine infarcts," *Circulation*. **92**, pp. 1902-1910, 1995.
12. R. Kim, E. L. Chen, J.A.C. Lima, R.M. Judd, "Myocardial Gd-DTPA kinetics determine MRI contrast enhancement and reflect the extent and severity of myocardial injury following acute reperfused infarction," *Circulation*. **94,** pp. 3318-3326, 1996.
13. C. Klein, S.G. Nekolla, F.M. Bengel, et al., "Assessment of myocardial viability with contrast-enhanced magnetic resonance imaging: comparison with positron emission tomography," *Circulation*. **105**, pp. 162-167, 2002.